Center for Turbulence Research
Proceedings of the Summer Program 1992

DNS and modeling of the interaction between turbulent premixed flames and walls

By T. J. Poinsot[1] AND D. C. Haworth[2]

The interaction between turbulent premixed flames and walls is studied using a two–dimensional full Navier–Stokes solver with simple chemistry. The effects of wall distance on the local and global flame structure are investigated. Quenching distances and maximum wall heat fluxes during quenching are computed in laminar cases and are found to be comparable to experimental and analytical results. For turbulent cases, it is shown that quenching distances and maximum heat fluxes remain of the same order as for laminar flames. Based on simulation results, a 'law–of–the–wall' model is derived to describe the interaction between a turbulent premixed flame and a wall. This model is constructed to provide reasonable behavior of flame surface density near a wall under the assumption that flame–wall interaction takes place at scales smaller than the computational mesh. It can be implemented in conjunction with any of several recent flamelet models based on a modeled surface density equation, with no additional constraints on mesh size or time step.

1. Introduction

The understanding and modeling of turbulent phenomena that occur near walls is a formidable task. Even in the absence of chemical reaction, building 'law–of–the–wall' models or low–Reynolds–number models is an ongoing research subject and no satisfactory practical solution is yet available for general use in engineering codes. The situation is even more difficult when a flame is present. Combustion is strongly influenced by the presence of walls which may cause flame fronts to quench, for example. Moreover, the flame has a significant effect on the flow in the vicinity of the wall as well as on the heat flux to the wall. For these reasons, modeling of flame–wall interactions in turbulent situations is an important issue. Still, few experimental or modeling results have been reported, and most present models for turbulent premixed combustion do not use any specific corrections for near–wall effects. At best this may result in errors in the prediction of the reaction rate and of the wall heat fluxes and temperatures. In some cases, the absence of any reasonable approximation of the wall effects leads to numerical difficulties and to the use of ad–hoc numerical corrections to obtain solutions. These corrections are based on pragmatic rather than on physical grounds. Our objective here is to explore the flame–wall interaction mechanisms at a fundamental level using direct numerical simulations (DNS). The understanding thus obtained provides a sound

1 C. N. R. S., Institut de Mecanique des Fluides de Toulouse, France
2 General Motors Research & Environmental Staff, Warren, MI

basis for a model which can be viewed as a law-of-the-wall approach for turbulent premixed combustion.

2. Flame-wall interaction in laminar flows

Before considering turbulent cases, it is useful to consider results obtained on wall quenching of laminar flames (Jarosinski 1986, Huang *et al.* 1986). For these flows, two important quantities have been introduced: the minimum distance between the flame and the wall δ_Q and the maximum heat flux Φ_Q through the wall during the interaction with the flame. Most authors normalize the wall distance y by a characteristic flame thickness $d = \lambda_1/(\rho_1 c_p s_l^0)$ and define the local Peclet number to be $P_e = y/d$ (Here a subscript '1' refers to reference properties in the fresh gases). Therefore, the quenching distance is often expressed by its Peclet number P_{eQ}: $P_{eQ} = \delta_Q/d$ (Huang *et al.* 1986, Vosen *et al.* 1984, Lu *et al.* 1990). The wall heat flux may be normalized by the laminar reference 'flame power' (heat release) to yield $\phi = \Phi_Q/(\rho_1 Y_F^1 s_l^0 \Delta H)$ where ρ_1 and Y_F^1 designate the fresh-gas density and fuel mass fraction, s_l^0 is the unstretched laminar flame speed, and ΔH is the heat of reaction ($Y_F^1 \Delta H = c_p(T_2 - T_1)$ if T_1 is the temperature of the fresh gases and T_2 is the adiabatic flame temperature). These two quantities may be correlated in laminar flows. If one assumes that at quenching, the wall heat flux Φ_Q is due to heat conduction in the gas layer of thickness δ_Q, one can write

$$\Phi_Q \simeq \lambda \frac{T_2 - T_w}{\delta_Q} , \tag{1}$$

where λ is the gas thermal conductivity and T_w is the wall temperature. From Eq. (1), we obtain a relation which is expected to hold when the wall heat transfer is dominated by diffusion:

$$\phi = \frac{T_2 - T_w}{T_2 - T_1} \frac{1}{P_{eQ}} . \tag{2}$$

Three typical situations have been studied in the past (Figure 1):

1. Head-on quenching

When a flame front reaches a cold wall ($T_w = T_1$) at a normal angle, head-on quenching (HOQ) occurs (Figure 1a). This case has been studied numerically and experimentally (Huang *et al.* 1986, Jarosinski 1986, Vosen *et al.* 1984). Results suggest that quenching occurs for Peclet numbers of the order of three. Heat flux measurements indicate values of ϕ of the order of 0.34, which is consistent with the value predicted by Eq. (2) with $P_{eQ} \approx 3$. In terms of simple physics, this result suggests that a flame stops propagating towards the wall when the heat losses to the wall are equal to about one-third of the nominal flame power. The fact that ϕ is almost constant for different fuels (Huang *et al.* 1986) suggests that the problem is thermally controlled and that simple chemistry may be used to compute this phenomenon.

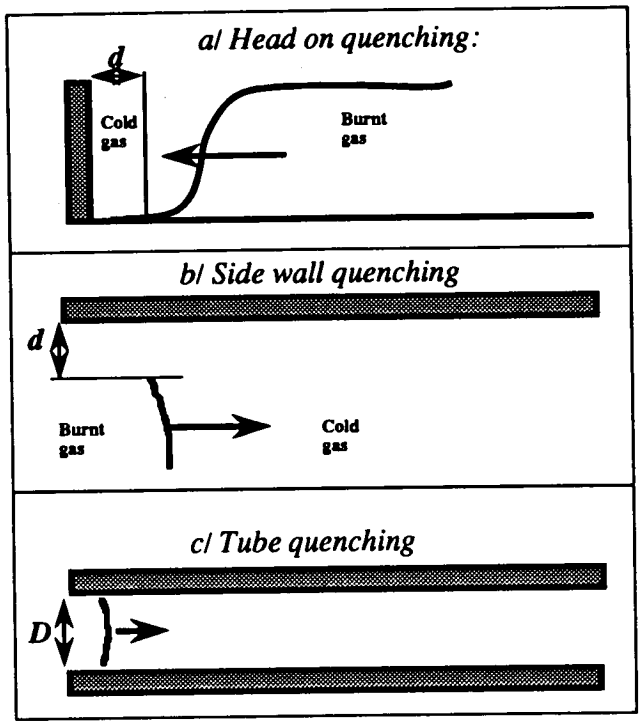

FIGURE 1. Configurations for flame–wall interaction studies in laminar flows.

2. Side–wall quenching

When a flame propagates parallel to a wall, the situation is different. Only localized quenching of the flame near the wall occurs (Figure 1b). This situation has been studied theoretically by Von Karman & Millan (1953) and Makhviladze & Melikov (1991), and experimentally by Lu *et al.* (1990) and Clendening *et al.* (1981). Peclet numbers in this case are of the order of seven suggesting values for ϕ of about 0.16 (Eq. (2)). Asymptotic theories of non–adiabatic flames also may be used to predict the quenching distance (Williams 1985): these predict the same order of magnitude for P_{eQ}.

3. Tube quenching

Total flame quenching may occur in a tube if its diameter is sufficiently small (Lewis & Von Elbe 1987, Jarosinski 1986, Fairchild *et al.* 1984) (Figure 1c). This phenomenon is exploited, for example, in the design of flame arrestors: these are ensembles of tubes with diameters smaller than the quenching distance so that a flame cannot propagate through them. Peclet numbers in this case are based on the tube diameter and are of the order of 50 (Aly & Hermance 1981). We will not consider this configuration here since in most practical situations, the dimensions of the system (e.g., the size of the combustor chamber) are too large to induce total quenching.

3. Numerical method and configuration

To study numerically how a laminar or a turbulent flame interacts with a cold wall we have utilized a DNS code developed at Stanford (Poinsot *et al.* 1991, Poinsot & Lele 1992). Since this code has been described elsewhere, we will recall only its principal features here. We consider a compressible viscous reacting flow. The chemical reaction is represented by a single-step mechanism, R (reactants) $\rightarrow$ P (products) where the reaction rate $\dot{w}_R$ is expressed as,

$$\dot{w}_R = B\rho Y_R \exp\left(-\frac{T_a}{T}\right). \tag{3}$$

This can be interpreted as a binary reaction where one of the reactants (Y_R) is always deficient. Following Williams (1985) we cast this expression in the form,

$$\dot{w}_R = \Lambda\rho Y_R \exp\left(\frac{-\beta(1-\Theta)}{1-\alpha(1-\Theta)}\right). \tag{4}$$

Here Θ is the reduced temperature $\Theta = (T - T_1)/(T_2 - T_1)$, and T_2 is the adiabatic flame temperature. The activation temperature is T_a and the coefficients Λ, α, and β are, respectively, the reduced pre-exponential factor, the temperature factor, and the reduced activation energy,

$$\Lambda = B\exp(-\beta/\alpha), \quad \alpha = (T_2 - T_1)/T_2, \quad \text{and} \quad \beta = \alpha T_a/T_2. \tag{5}$$

Fluid properties follow the equations,

$$\rho = \rho_1(pT_1/p_1T)\ ,\ \mu = \mu_1(T/T_1)^b\ ,$$

$$Le = \lambda/\rho D c_p = \text{constant}\ ,\ Pr = \mu c_p/\lambda = \text{constant}\ , \tag{6}$$

where μ, λ, and D are molecular diffusivities of momentum, internal energy, and species, respectively, and b is a constant. Using these assumptions and a Cartesian frame of reference, the conservation equations for compressible flows are solved using a high-order finite difference scheme (Lele 1992).

The calculations are initialized with reactants on one side of the computational domain and products on the other; these are separated by a laminar premixed flame. The wall is located on the reactant side of the domain (Figure 1a). All velocity components are zero on the wall and the wall temperature is imposed. For all the cases shown here, the wall temperature is equal to the fresh gas temperature, T_1. On lateral boundaries, periodic conditions are enforced. On the right-hand side of the domain, non-reflecting boundary conditions are used (Poinsot & Lele 1992).

The initial velocity field (turbulence spectrum) and spatial distribution of reactant mass fraction are specified at $t = 0$: the system is then allowed to evolve in time. The initially planar flame is convected and strained by the turbulence while the combustion influences the fluid mechanics through dilatation and temperature-dependent properties (Eq. (6)). After some time (typically 5 to 20 flame times in these computations), the flame reaches the wall and begins to interact with it.

4. Diagnostics

In the present case, we are especially interested in the effect of the wall on the flame structure. Postprocessing of the two–dimensional computed fields (snapshots at fixed times) begins by defining a flame front as an isocontour of temperature T. Once the flame front has been located, the local normal and local flame curvature are readily computed; curvature is taken to be positive for flame elements that are concave towards the products and conversely for elements concave towards reactants. One–dimensional cuts normal to the flame are taken: it is these profiles that define the local 'structure' of the turbulent flame. We compare the local turbulent flame profiles with the steady one–dimensional laminar flame profile for the same chemistry and fluid properties. Of particular interest is the distribution along the flame of the normalized local flame speed ('flamelet speed') s_n defined by $s_n = \int \dot{w}\, dn \,/\, s_l^0$, that is, the integral of the reaction rate profile in a direction locally normal to the flame.

The fixed chemical parameters used for this study are summarized in Table I. The flame speed and thickness are normalized respectively by the sound speed c and by the reference length $d = \lambda_1/(\rho_1 c_p s_l^0)$. The flame thermal thickness δ_l^0 is based on the maximum temperature gradient: $\delta_l^0 = (T_2 - T_1)/Max(\frac{\partial T}{\partial n})$.

Table I. Fixed parameters for DNS of flame–wall interaction.

α	β	Λ	b	Pr	Le	s_l^0/c	δ_l^0/d
0.75	8.00	146.	0.76	0.75	1.0	0.016	3.8

5. DNS of the interaction between a laminar flame and a wall

To check the accuracy of the model, laminar runs were performed first. Figure 2 presents time variations of the flame distance to the wall as well as the flame power $\rho_1 s_n c_p (T_2 - T_1)$ and the normalized wall heat flux ϕ. There time has been normalized by the flame time $t_F = \delta_l^0/s_l^0$ and y is the distance from the wall. The values obtained from DNS for this case are $P_{eQ} = 3.4$ and $\phi = 0.36$. These values are in good agreement with experimental data (Lu *et al.* 1990, Vosen *et al.* 1984) and with the simple model given by Eq. (2). Although total quenching occurs at $P_{eQ} = 3.4$, the flame senses the presence of the wall before this time: the flame speed s_n begins to decrease when the wall distance is less than a distance δ_T given by $P_e = \delta_T/d \approx 8$. Therefore, two zones are necessary to describe the near-wall region:

(i) The 'quenching' zone stretches from the wall to a local Peclet number y/d of about 3.5 ($0 < y < \delta_Q$). In this zone, no reaction ever takes place.

(ii) The 'influence' zone goes from the wall to a Peclet number y/d of about 8 ($0 < y < \delta_T$). Any flame entering the influence region will start sensing the wall and will eventually get quenched. The time t_Q needed for the flame to quench after it enters the influence zone is of the order of two flame times, $t_Q = 2t_F = 2\delta_l^0/s_l^0$.

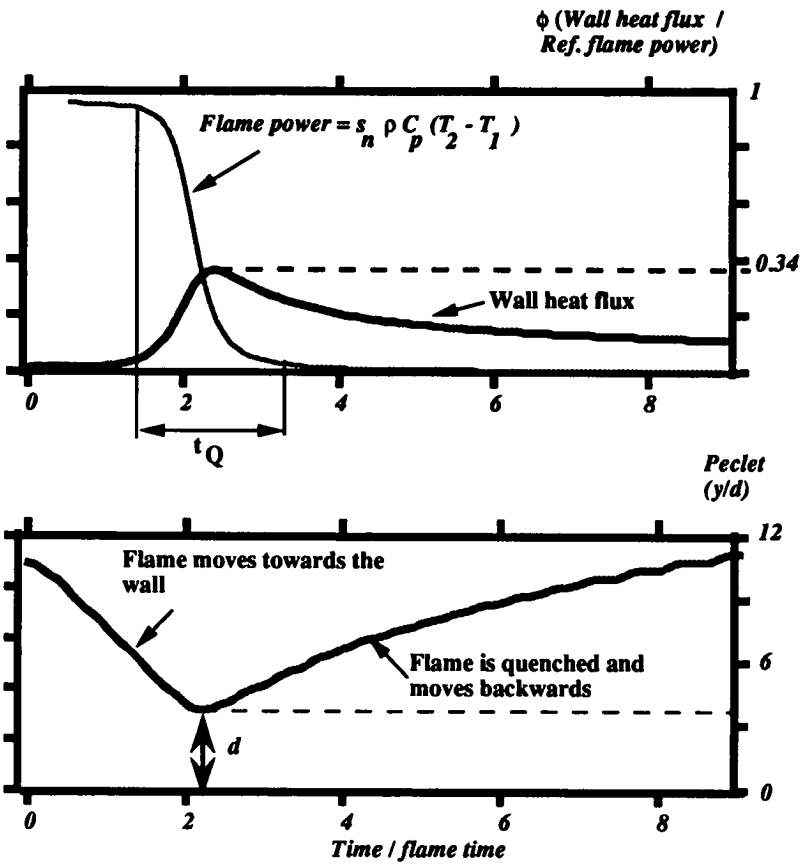

FIGURE 2. Numerical results for a laminar flame–wall interaction.

6. DNS of the interaction between a turbulent flame and a wall

The interaction between the wall and a turbulent flame front is characterized by three effects:

(i) A local thermal effect, by which heat losses to the wall affect the flame structure and result in local quenching.

(ii) A geometrical effect which limits the spatial extent of the flame brush and reduces the flame–brush size in the vicinity of the wall.

(iii) A laminarization effect which is an indirect effect of the wall on the flame. The wall affects the structure of the turbulence and leads to laminarization immediately adjacent to the wall. This induces a strong decrease of the turbulent stretch and thereby a decrease of the flame area.

Preferential species diffusion is beyond the scope of the present simple-chemistry investigation.

The structure of turbulence near the wall is clearly an important issue in the latter two questions. The configuration studied here corresponds to the 'shear-free' boundary layer in which turbulence with no mean shear interacts with a wall. This

may be realized experimentally in a wind tunnel, for example, using walls that move at the mean flow speed. The shear–free boundary layer has been studied experimentally by Thomas & Hancock (1977) and Uzkan & Reynolds (1967), theoretically by Hunt & Graham (1978), and numerically by Biringen & Reynolds (1981). The flow structure can be summarized as follows. Starting from initially isotropic homogeneous turbulence, the wall induces a perturbation zone whose thickness increases with time. In this zone, viscous effects are important, and the turbulence is damped. Moreover, by imposing zero normal velocities, the wall increases velocity perturbations in planes parallel to the wall (at sufficiently high Reynolds numbers). The role of this near–wall turbulence structure on flame evolution is difficult to quantify in the present simulations. We will concentrate instead on the thermal effects.

The parameters for the simulations reported here are summarized in Table II. There u' is the rms turbulence velocity, L_i is the length scale of the most energetic vortices in the initial turbulence spectrum, and l is the turbulence integral scale based on two–point velocity correlations. The initial turbulence field was chosen to produce small–scale turbulence near the wall and to impose zero velocity fluctuations at the wall. More sophisticated (three–dimensional) approaches will be necessary to produce more general results.

Table II. Initial conditions for DNS of turbulent flame–wall interaction.

Case	u'/s_l^0	L_i/δ_l^0	l/δ_l^0	$Re_l = u'l/\nu$	$Re_L = u'L_i/\nu$
2*D*3	6.25	8.9	2.85	90	280
2*D*4	6.25	4.5	1.43	45	140
2*D*6	6.25	1.9	0.64	19	60

Figures 3 and 4 present snapshots at one instant in time of reaction rate and vorticity fields during the interaction between the turbulent flame and the wall. Time has been normalized by the flame time $t_F = \delta_l^0/s_l^0$, and the maximum value of the vorticity modulus is normalized by the characteristic flame strain s_l^0/δ_l^0. The structure of the vorticity field is affected both by the flame (viscosity in the burnt gases dissipates vorticity rapidly) and by the wall (the normal velocity component close to the wall goes to zero while the parallel component increases). Vortex pairs appear to play a dominant role. In Figures 3 and 4, for example, one vortex pair attracts a part of the flame front towards the wall while another pair pushes a different part of the flame away from the wall (sequence $t/t_F = 4.4$ to $t/t_F = 6.6$). This is confirmed by Figure 5 which presents the time evolution of the minimum and maximum wall distances in terms of Peclet numbers. When the first flame element touches the wall at time $t/t_F \simeq 6$, the most distant element is moving away from the flame front. This ejection of flame elements away from the flame

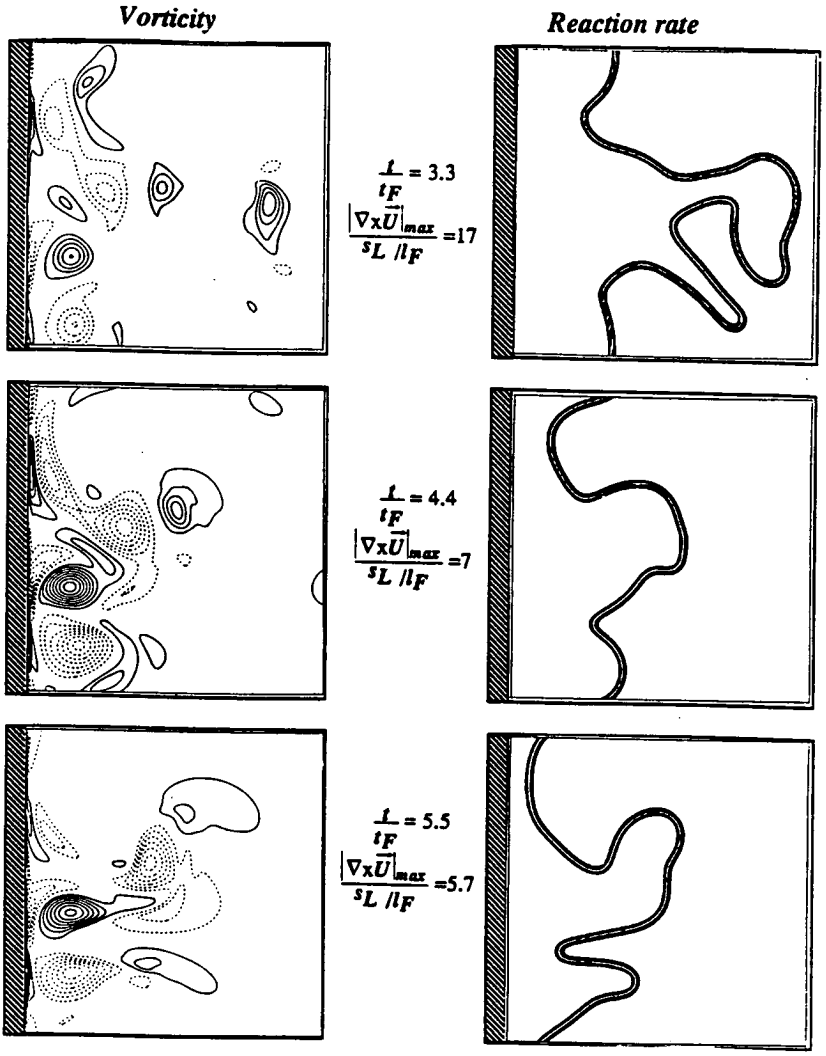

FIGURE 3. Vorticity and reaction rate contours for a turbulent flame–wall interaction (Case 2D4). Solid lines denote clockwise vorticity, dashed lines denote counterclockwise.

front may induce local counter–gradient turbulent diffusion of flame surface density which might be important in modeling.

As far as the thermal effect is concerned, results obtained during this simulation and during other simulations of the same type lead to a simple result (Figure 6): the maximum local heat flux to the wall corresponds within 10 percent to the laminar heat flux ($\phi = 0.36$), and the quenching distance δ_Q is equal to the value obtained in laminar cases ($P_{eQ} = 3.4$). Although the initial conditions used for these simulations lead to large velocity perturbations near the wall, the heat flux to the wall appears to be controlled mainly by heat diffusion, and the local instantaneous maximum

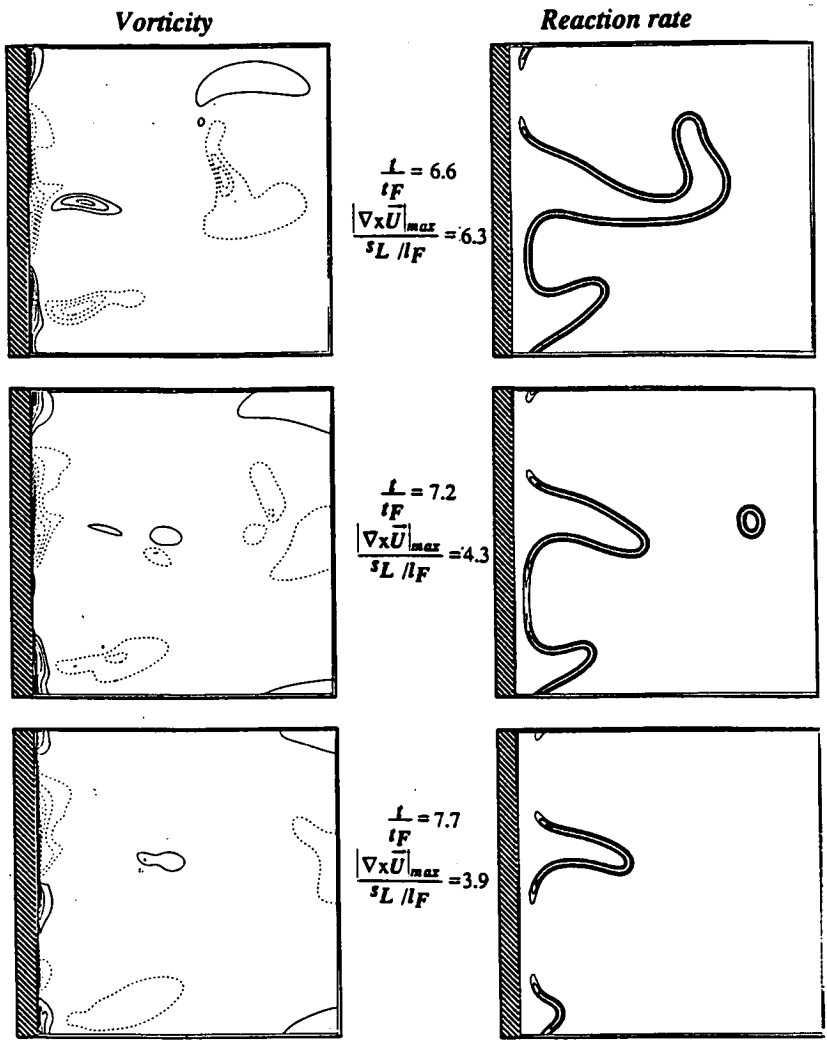

FIGURE 4. Vorticity and reaction rate contours for a turbulent flame–wall interaction (Case 2D4, continued).

heat flux obtained during quenching is the same as for the laminar cases.

Figure 7 presents a scatter plot of normalized flamelet speed s_n versus distance to the wall. This plot exhibits different behaviors for different flame elements ('flamelets') as they approach the wall. No flame elements approach closer than the laminar quenching distance δ_Q to the wall, and the minimum Peclet number is equal to about 3.5. Branch 1 corresponds to flames reaching the wall at normal angles (head–on quenching): these follow the curve (solid line) predicted by the laminar HOQ computation (Section 5), quenching at a Peclet of close to 3.5. Branch 2 corresponds to flamelets which disappear at Peclet numbers of about 7. Examination of DNS fields for these points suggest that these flamelets are propagating

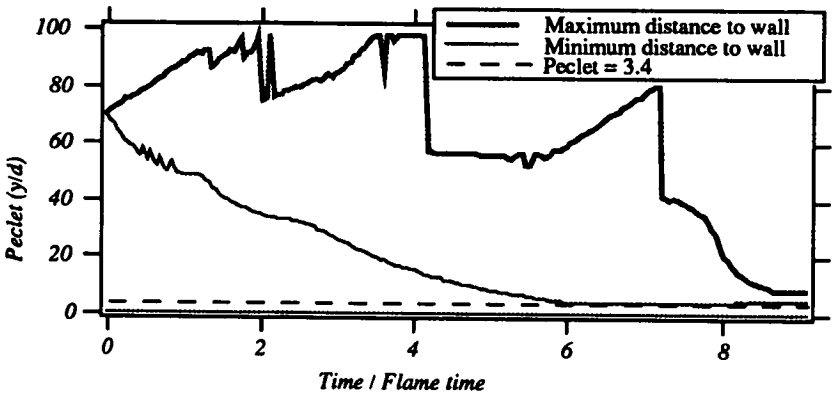

FIGURE 5. Maximum and minimum (over all computational cells adjacent to the wall) flame–wall distances for Case 2D4.

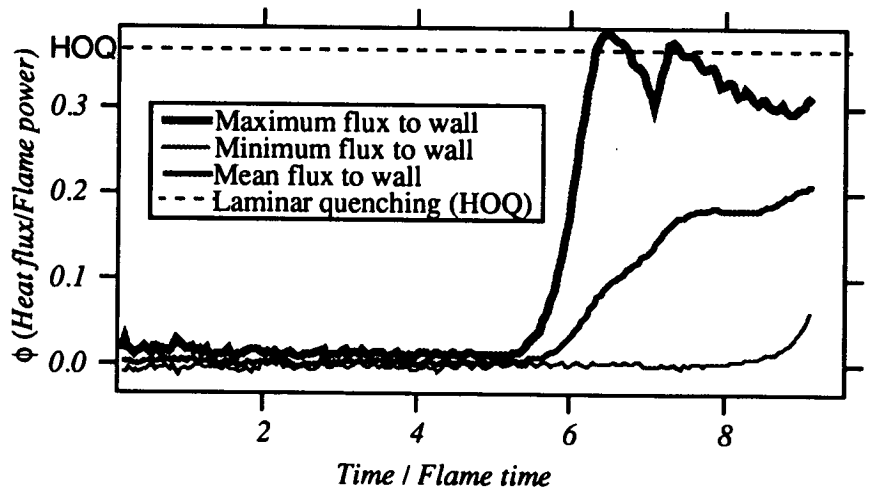

FIGURE 6. Minimum, maximum, and mean (over all computational cells adjacent to the wall) wall heat fluxes for Case 2D4.

parallel to the wall and not towards the wall, thus corresponding to the side-wall quenching situations described in Section 2. Branch 3 corresponds to flamelets which burn faster (accelerate) as they approach the wall, but subsequently quench on reaching a Peclet of about 3.5. At this point, no explanation for Branch 3 is proposed. The number of flamelets following Branch 2 is small compared to the other branches: most flamelets reach the wall at a normal angle. This is confirmed

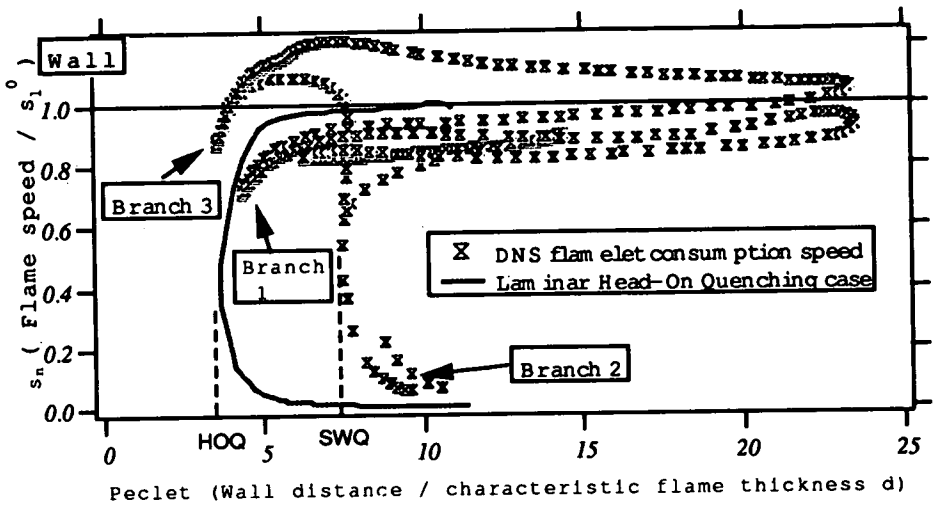

FIGURE 7. Flamelet consumption rate s_n versus wall distance at time $t/t_F = 4$ (Case 2D6).

by the distributions of flame curvature presented in Figure 8. While the flame is still far from the wall ($t/t_F = 0.5$), the mean curvature conditioned on distance to the wall is almost symmetrical about zero. As the flame brush approaches the wall ($t/t_F = 4$), flamelets flatten and curvature diminishes. Furthermore, positive values of curvature are clipped more strongly than negative values indicating that flamelets are predominantly concave towards the fresh gases and that most of them will reach the wall at close to a normal incidence angle.

The distance at which flamelets begin to sense the presence of the wall (i.e., where their local flamelet speed begins to drop) is given by a Peclet number of the order of 10 (Figure 7), close to that found for the laminar simulations. Although the existence of the three different branches suggests a more complex pattern than simple head-on quenching, it appears that an influence zone may be defined for turbulent cases whose thickness (in Peclet number) is something close to 10.

It appears that both the quenching zone thickness (δ_Q) and the influence zone thicknesses (δ_T) have similar values for turbulent and laminar premixed flames. This has some important consequences. Consider, for example, a reacting boundary layer. Invoking the usual normalizations, we denote by a superscript $^+$ a wall-units-scaled value: $y^+ = yu_\tau/\nu$, where u_τ is the friction velocity and ν is the kinematic viscosity. The edge of the quenching zone is located at $\delta_Q^+ = u_\tau \delta_Q/\nu = (P_{eQ}/Pr)(u_\tau/s_l^0)$. For most practical situations, u_τ (1 to 5 m/s) is of the order of the flame speed s_l^0 (0.3 to 1.5 m/s) so that δ_Q^+ is of the order of 1 to 10. That means that the quenching zone is located inside the viscous layer. Flamelets travelling from the free stream towards the wall *first* encounter laminar flow in the viscous

region and only *later* are quenched. This result will be used in the modeling of the flame–wall interaction (Section 7).

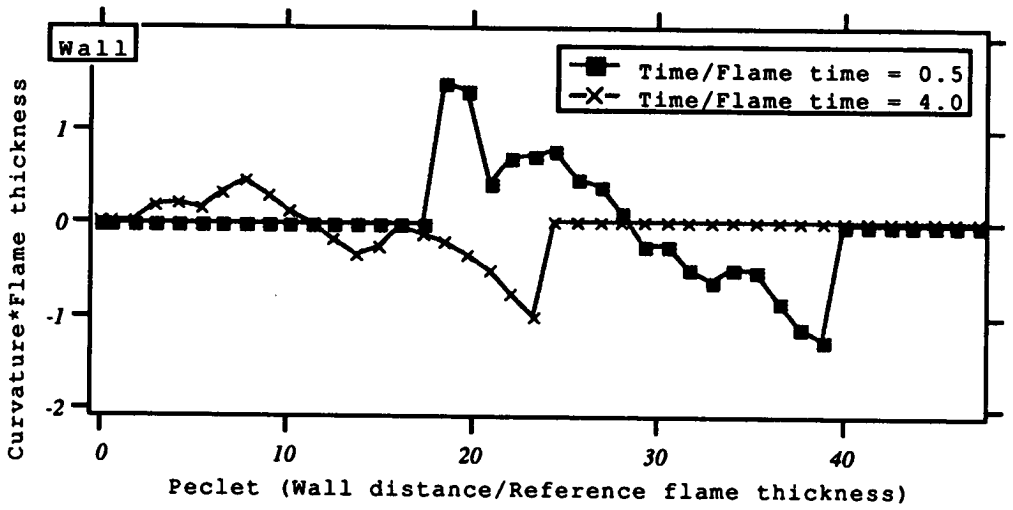

FIGURE 8. Mean curvature (conditioned on wall distance) for a flame far from the wall ($t/t_F = 0.5$) and a flame reaching the wall ($t/t_F = 4$) (Case 2D6).

7. A law–of–the–wall for turbulent premixed combustion

From the previous results, it is possible to construct law–of–the–wall models for premixed turbulent flames which we will designate here as 'FIST' models (Flame Interacting with Surface and Turbulence). This model will be derived in the framework of flamelet models: the dependent variable which will be modeled is the flame surface density (surface–to–volume ratio) Σ as defined by Pope (1988). Implementation is discussed in the context of a finite–volume method, although the concept may be applied to other numerical approaches.

We consider a generic flamelet model in which the flame surface density Σ evolves according to,

$$\frac{\partial \Sigma}{\partial t} + \frac{\partial \overline{U_i} \Sigma}{\partial x_i} = \frac{\partial \mathcal{F}_i}{\partial x_i} + S - D - D_Q. \tag{7}$$

This equation includes transport, turbulent diffusion ($\mathcal{F}_i$), and source (S) and consumption terms (D, D_Q). With the exception of the D_Q term which represents thermal quenching due to the wall, several recent flamelet models can be cast into this form (Cant *et al.* 1990, Candel *et al.* 1988, Boudier 1992, Cheng & Diringer 1991). The development of the present FIST model is independent of the exact

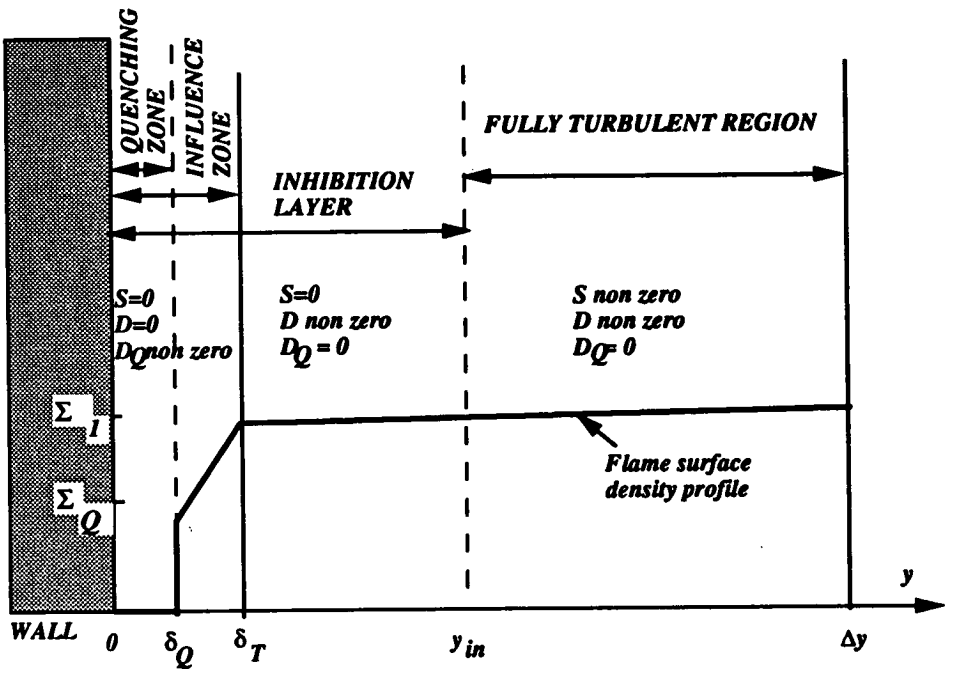

FIGURE 9. Principle of the FIST model (law-of-the-wall model for premixed turbulent combustion).

form of the S and D terms. The assumptions which will be used are the following (see Figure 9):

- We will consider a situation where a law-of-the-wall approach is used to describe near-wall turbulence since this is the case for most practical codes based on Reynolds-averaged mean equations.

- The computational cell size adjacent to the wall Δy is larger than the quenching zone and larger than the zone over which the wall modifies the free-stream turbulence structure (typically, in the case of a turbulent boundary layer, the first grid point is located at a y^+ larger than 200).

- Outside the quenching zone ($y > \delta_T$), no thermal quenching occurs as shown by DNS (see Section 6) so that $D_Q = 0$.

- Inside the quenching zone ($0 < y < \delta_T$), we need to estimate the characteristic time t_Q at which flamelets are quenched. For laminar cases, t_Q is of the order of two flame times as evidenced by DNS for laminar flames (see Section 5). Despite the existence of the three branches shown in Section 6, we will assume that all flamelets entering the influence zone in the turbulent case are quenched on a time

scale $t_Q = 2t_F$. Therefore, D_Q may be written as $D_Q = \Sigma_Q/t_Q$ where Σ_Q is the mean flame surface density in the quenching layer. This thermal quenching effect is supposed to be stronger than the usual consumption terms (due to mutual annihilation) in the Σ equation so that D may be set to zero. Since there is no turbulence inside the quenching layer (see Section 6) we will also assume that there are no source terms in this zone ($S = 0$).

– Inside an 'inhibition zone' which extends from $y = 0$ to $y^+ = y^+_{in}$, we assume that turbulence is affected strongly enough by the wall to reduce the flame stretch to zero. This assumption is not based on the present DNS but rather on the observation that turbulence must be strongly damped in this zone, therefore reducing the turbulent stretch.

– In the rest of the first computational cell ($y^+_{in} < y^+ < \Delta y^+$), the normal form of the flamelet model is used.

– Finally, for the sake of clarity, we will consider a situation where the flow is homogeneous in planes parallel to the wall (i.e., Σ is a function of y only), and we will also neglect mean velocities normal to the wall. These last assumptions allow mean convective terms ($\frac{\partial \overline{U_i}\Sigma}{\partial x_i}$) to be neglected in the finite–volume expression of Eq. (7). This assumption is not restrictive, and is invoked only for convenience in writing the resulting modeled equations.

Under the previous assumptions, the equations of a FIST model may be derived by integrating Eq. (7) in two zones: the influence zone and the rest of the first computational cell. The mean flame surface densities in the influence zone and in the first computational cell, respectively, will be defined by: $\Sigma_Q = \frac{1}{\delta_T}\int_0^{\delta_T} \Sigma dy$, and $\Sigma_1 = \frac{1}{\Delta y - \delta_T}\int_{\delta_T}^{\Delta y} \Sigma dy$.

In the quenching zone, terms S and D are small compared to the thermal quenching effect. When Eq. (7) is integrated between $y = 0$ and $y = \delta_T$ with this assumption, the following conservation equation for Σ_Q is obtained:

$$\frac{\partial \Sigma_Q}{\partial t} = \frac{\mathcal{F}(y = \delta_T)}{\delta_T} - \frac{\Sigma_Q}{t_Q} \,. \tag{8}$$

Integrating Eq. (7) between $y = \delta_T$ and $y = \Delta y$ provides an evolution equation for the average flame surface density Σ_1 in this zone:

$$\frac{\partial \Sigma_1}{\partial t} = \frac{1}{\Delta y - \delta_T}(\mathcal{F}(y = \Delta y) - \mathcal{F}(y = \delta_T)) + S(1 - \frac{y^+_{in} - \delta_T}{\Delta y}) - D \,. \tag{9}$$

Equations (8) and (9) form a closed set which provides the flame surface density in the quenching region (Σ_Q) and in the first computational cell (Σ_1). These two equations state that there is a sink mechanism for flame surface in the first computational cell: flamelets diffuse towards the quenching zone ($\mathcal{F}(y = \delta_T)$ term in Eq. (9)) and later get quenched in this zone on the time scale t_Q.

8. An equilibrium formulation for FIST models

Although Eqs. (8) and (9) may be solved under this form in finite–volume codes, it is interesting to propose a simpler model 'Equilibrium FIST' in which the flame

surface density in the quenching region Σ_Q may be eliminated. In the Equilibrium FIST model, four additional assumptions are invoked:

– The turbulent diffusion term $\mathcal{F}_i$ is written as $\mathcal{F}_i = \frac{\nu_t}{S_c}\frac{\partial \Sigma}{\partial x_i}$ where ν_t is a turbulent diffusion coefficient and S_c is a turbulent Schmidt number.

– The flame surface–density profile inside the quenching zone is supposed to exhibit strong spatial variations compared to the profile outside this zone. Then the diffusion term $\mathcal{F}_y(y = \delta_T)$ may be estimated by $\mathcal{F}_y(y = \delta_T) = E\frac{\nu_t}{S_c}\frac{\Sigma_1 - \Sigma_Q}{\delta_T}$ where E is a model constant of order unity.

– The quenching zone is assumed to be in equilibrium, i.e., diffusion balances dissipation in Eq. (8). This allows us to derive an explicit expression for the flame surface density in the quenched region as a function of the flame surface density in the first cell Σ_1:

$$\Sigma_Q = \Sigma_1 \frac{a_Q}{a_Q + 1} \quad \text{where} \quad a_Q = E\frac{\nu_t}{S_c}\frac{t_Q}{\delta_T^2} \,. \tag{10}$$

The parameter a_Q is proportional to the turbulent diffusivity ν_t normalized by the quenching time and distance.†

– The size of the first cell is supposed to be sufficiently large compared to the quenching distance ($\Delta y >> \delta_T$) to neglect δ_T in the RHS of Eq. (9).

Under these assumptions, the Equilibrium FIST model provides the following conservation equation for the flame surface density Σ_1 near a wall:

$$\frac{\partial \Sigma_1}{\partial t} = \frac{1}{\Delta y}\mathcal{F}(y = \Delta y) - \frac{\delta_T}{\Delta y}\frac{a_Q}{a_Q + 1}\frac{\Sigma_1}{t_Q} + S(1 - \frac{y_{in}^+}{\Delta y}) - D \,. \tag{11}$$

Wall corrections appear here only as an additional diffusion term towards the wall (second term on right–hand side of Eq. (11)) and as a correction of the turbulent stretch $S(1 - y_{in}^+/\Delta y)$. All other terms may be estimated by classical finite–volume methods. In this model, some constants may be set directly from the present DNS results: the influence distance is given by $\delta_T = P_e d = P_e \frac{\lambda_1}{\rho_1 c_p s_l^0}$ where the Peclet number should be of order 10 (Sections 5 and 6), and the quenching time scale t_Q is given by $t_Q = 2t_F = 2l_F^0/s_l^0$ (Section 5). The parameter y_{in}^+ has not been estimated from the present DNS results but might be determined by using a three–dimensional boundary–layer code. Reasonable estimates for this quantity are of the order of 50. The turbulent diffusivity ν_t appearing in the above formula may be estimated using standard expressions for this quantity near walls. Further improvements of the model may be based on an expression for ν_t which would take into account the counter-gradient diffusion of Σ mentioned in Section 6.

The simplicity of this formulation allows it to be used in conventional Reynolds–averaged multidimensional flow codes without additional constraints on time step

† By using an eddy–viscosity concept near the wall ($\nu_t = Ku'\delta_T$), a_Q may be interpreted as a ratio between turbulence velocity near the wall and a characteristic quenching velocity ($a_Q = K\frac{E}{S_c}\frac{u'}{\delta_T/t_Q}$).

or grid size. Although the approach simplifies the actual physics of flame–wall interaction, it represents a significant improvement over approaches which fail to account explicitly for the influence of the wall on the turbulent flame. The Equilibrium FIST model accounts for turbulent diffusion of flamelets towards the wall and quenching on a time scale which is given by DNS. It also accounts in a crude way for the laminarization effect of the wall up to a distance given by y_{in}^{+}.

9. Conclusions

Calculations of premixed laminar and turbulent flames interacting with isothermal walls have been reported. Quantitative results have been presented illustrating the influence of distance from the wall on the local and global flame structure. For laminar cases, the computed minimum distance between wall and flame (the 'quenching distance') and the maximum wall heat flux during quenching have been found to be comparable with available experimental and analytical results. For turbulent cases, it has been shown that quenching distances and maximum heat flux remain of the same order as for laminar flames. Correlations between wall distance and flame structure suggest that thermal effects are important only very close to the wall and that the wall acts as a strong sink term for flame surface density. Based on these DNS results, a model has been proposed to take into account the interaction between the turbulent flame and the wall. The equilibrium version of this model may be implemented in conventional finite–volume codes together with flamelet models based on modeled surface density equations. Further tests are necessary to assess its performance.

An important extension of the FIST model would be the development of a model for wall heat flux. Such a model could be based on the knowledge of the flame surface density in the quenching zone and on the correlations between wall heat flux and flame position. This issue will be addressed in future work.

REFERENCES

ALY, S. L. & HERMANCE, C. E. 1981 A two–dimensional theory of laminar flame quenching. *Combust. & Flame.* **40,** 173–185.

BIRINGEN, S. & REYNOLDS, W. C. 1981 Large–eddy simulation of the shear–free turbulent boundary layer. *J. Fluid Mech.* **103,** 53–63.

BOUDIER, P. 1992 Modelisation de la combustion turbulente dans un moteur piston. Ph.D. Thesis, Ecole Centrale, Paris.

CANDEL, S. M., MAISTRET, E., DARABIHA, N., POINSOT, T., VEYNANTE, D. & LACAS, F. 1988 Experimental and numerical studies of turbulent ducted flames. *Marble Symposium, CALTECH.* 209–236.

CANT, R. S., POPE, S. B. & BRAY, K. N. C. 1990 Modeling of flamelet surface to volume ratio in turbulent premixed combustion. *23rd Symp. (Intl.) on Combust.* The Combustion Institute, Pittsburgh, 809–815.

CHENG, W. K. & DIRINGER, J. A. 1991 Numerical modeling of SI engine combustion with a flame sheet model. SAE Paper No. 910268.

CLENDENING, J. C. W., SHACKLEFORD, W. & HILYARD, R. 1981 Raman scattering measurement in a side wall quench layer. *18th Symp. (Intl.) on Combust.* The Combustion Institute, Pittsburgh, 1583–1589.

FAIRCHILD, P. W., FLEETER, R. D. & FENDELL, F. E. 1984 Raman spectroscopy measurement of flame quenching in a duct type crevice. *20th Symp. (Intl.) on Combust.* The Combustion Institute, Pittsburgh, 85–90.

HUANG, W. M., VOSEN, S. R. & GREIF, R. 1986 Heat transfer during laminar flame quenching, effect of fuels. *21st Symp. (Intl.) on Combust.* The Combustion Institute, Pittsburgh, 1853–1860.

HUNT, J. C. R. & GRAHAM, J. M. R. 1978 Free-stream turbulence near plane boundaries. *J. Fluid Mech.* **84,** 209–235.

JAROSINSKI, J. 1986 A survey of recent studies on flame extinction. *Combust. Sci. & Technol.* **12,** 81–116.

LELE, S. 1992 Compact finite difference schemes with spectral-like resolution. *J. Comput. Phys.* (to appear).

LEWIS, B. & VON ELBE, G. 1987 *Combustion, Flames and Explosions of Gases.* Academic Press, New York.

LU, J. H., EZENKOYE, O., GREIF, R. & SAWYER, F. 1990 Unsteady heat transfer during side wall quenching of a laminar flame. *23rd Symp. (Intl.) on Combust.* The Combustion Institute, Pittsburgh, 441–446.

MAKHVILADZE, G. M. & MELIKOV, V. I. 1991 Flame propagation in a closed channel with cold side wall. *UDC.* **536.46,** 176–183. (*Fizika Goreniya i Vzryva* **2** 49–58, March–April 1991).

POINSOT, T. & LELE, S. 1992 Boundary conditions for direct simulations of compressible viscous flows. *J. Comp. Phys.* **101,** 104–129.

POINSOT, T., VEYNANTE, D. & CANDEL, S. 1991 Quenching processes and premixed turbulent combustion diagrams. *J. Fluid Mech.* **228,** 561–605.

POPE, S. 1988 The evolution of surfaces in turbulence. *Intl. J. Engng. Sci.* **26,** 445–469.

THOMAS, N. H. & HANCOCK, P. E. 1977 Grid turbulence near a moving wall. *J. Fluid Mech.* **82,** 481–496.

UZKAN, T. & REYNOLDS, W. C. 1967 A shear-free turbulent boundary layer. *J. Fluid Mech.* **28,** 803–821.

VON KARMAN, T. & MILLAN, G. 1953 Thermal theory of laminar flame front near cold wall. The Combustion Institute, Pittsburgh, 173–177.

VOSEN, S. R., GREIF, R. & WESTBROOK, C. K. 1984 Unsteady heat transfer during laminar flame quenching. *20th Symp. (Intl.) on Combust.* The Combustion Institute, Pittsburgh, 76–83.

WILLIAMS, F. A. 1985 *Combustion theory.* B. Cummings, Menlo Park, CA, 73–76.